J. Basic. Appl. Sci. Res., 3(2s)653-665, 2013
© 2013, TextRoad Publication

ISSN 2090-4304
Journal of Basic and Applied Scientific Research
www.textroad.com

A Numerical Simulation of Mixed Radiation and Forced Convective Heat Transfer in a Lid-Driven cavity Filled with Participating Media

Mohammad Mehdi Keshtkar

Assistant Professor of Mechanical Engineering, Islamic Azad University, Kerman Branch, Iran,

Received: June 10 2013
Accepted: July 10 2013

ABSTRACT

A numerical study has been performed to investigate the combined radiation and forced convection heat transfer characteristics of participating medium contained in a lid-driven cavity. All of the walls are kept at constant but with different temperatures. The upper horizontal wall moves on its own plane from left to right side at constant speed while all other walls are fixed. Combustion in lid-driven cavity is modeled by considering a non-uniform heat generation zone with parabolic distribution. The transport equations for unsteady laminar flow are solved numerically with finite difference method and the discrete ordinates method (DOM) is used to model the radiative transfer in absorbing-emitting and scattering media. The heat transfer characteristics inside the cavity are presented in the form of isotherms for various values of the Reynolds number at different time steps. In addition, the influences of many important parameters, namely, Reynolds number, location of the heat generation zone and the scattering albedo on thermal behavior of the participating medium are studied. Also, the variations of radiative and total heat fluxes on the walls at different Reynolds numbers are also presented to show the overall heat transfer characteristics inside the cavity. The present results are compared with some reported theoretical results by other investigators and good agreement is found.

KEYWORDS: radiation, forced convection, lid-driven cavity, discrete ordinates method, heat generation zone.

1. INTRODUCTION

Combined heat transfer phenomenon occurs in many engineering systems such as solar collectors, drying technology, cooling of electronic devices, flat glass manufacturing and nuclear reactors. The cavity with moving lid is one of the most important applications of such mechanism, which is seen in cooling of electronic chips and food industry (aluria et al., 1986). In the literature, a lot of works have been done over the last three decades in the area of numerical and experimental combined heat transfer. Mixed convective flow in a bottom heated square driven cavity was numerically studied and the effect of Prandtl number on the flow and heat transfer process investigated (Moallemi et al., 1992). At this work, found that the effects of buoyancy are more pronounced for higher values of the Prandtl number. They also derived a correlation for the average Nusselt number in terms of the Prandtl number, Reynolds number, and Richardson number. A numerical and experimental study on steady flow in rectangular two sided lid-driven cavities carried out (Kuhlmann et al., 1997). They found that the basic two-dimensional flow is not always unique. A problem of unsteady laminar mixed convection flow and heat transfer of an electrically conducting and heat generating in a vertical lid-driven cavity at the presence of a magnetic field examined (Chamkha, 2002). A numerical and an experimental study on transient mixed convection in a lid-driven enclosure have been investigateded (Ji et al., 2007). The authors showed that the temperature field exhibits weak fluctuating behavior at early times in the mid and upper portion of the cavity. The heat transfer enhancement in a two-dimensional enclosure utilizing nanofluids for a wide range of Grashof number and volume fraction was investigated (Khanafer et al., 2003). It was found that the heat transfer across the enclosure increases with increasing in the volumetric fraction of the copper nanoparticles in water for different Grashof number. A numerical investigation of natural convection in an enclosure consisting of two isothermal horizontal wavy walls and two adiabatic vertical straight walls was conducted (Das et al., 2003). Laminar flow through a two-dimensional square cavity with internal heat generation by numerical techniques was analyzed (Buscaglia et al., 2003). Mixed convection in rectangular cavities at various aspect ratios with moving isothermal side walls and constant heat flux on the bottom wall was performed (Gau et al., 2004). Convection flow in two-sided lid-driven differentially heated square cavity with three cases (according to the direction of the lid movement) was numerically investigated and it was found that the ratio of heat transfer is larger when the vertical walls move in opposite directions, whereas if the walls move in the same direction the lid opposing buoyancy forces decreases the heat transfer significantly (Oztop et al., 2004). Mixed convection heat transfer in lid-driven cavity with a sinusoidal wavy bottom surface was investigated (Al-Amiri et al., 2007). Their findings showed that the corrugated lid-driven cavity could be considered as an effective heat transfer mechanism at larger wavy surface amplitudes and low Richardson number. An experimental study of assisted and opposed air flows through a vertical circular tube under uniform wall heat flux to investigate the effects of flow direction and the tube inclination angles on the heat transfer characteristics of laminar mixed convection flow was carried out (Mohammed, 2008). He concluded that for opposed flow, the variation of the surface temperature is strongly dependent on the Reynolds and Grashof numbers. The heat transfer enhancement in a differentially heated enclosure using variable thermal conductivity and variable viscosity of Al2O3–water and Cu–water nanofluids was investigated (Abu-Nada et al., 2010). The problem of natural convection cooling of a localized heat source at the bottom of a nanofluid filled enclosure was discussed (Aminossadati et al., 2009). The effect of thermal radiation and magnetic field on flow and heat transfer over an unsteady stretching surface in a micropolar fluid was investigated (Aldawody et al., 2011). The combined influences of viscous dissipation, joule heating, temperature-dependent viscosity, on the time-

* **Corresponding Author**: Mohammad Mehdi Keshtkar, Assistant of Mechanic, Islamic Azad University, Kerman Branch, Iran mkeshtka54@yahoo.com.

dependent MHD permeable flow having variable viscosity analyzed (Turkyilmazoglu, 2011). The forced convection of laminar nanofluid in a microchannel with both slip and no-slip conditions studied numerically (Raisi et al., 2011). They showed that the heat transfer rate is significantly affected by the solid volume fraction and slip velocity coefficient at high Reynolds numbers. A problem on natural convection laminar flow in a partially side heated square cavity with internal heat generation investigated numerically by employing Finite Element Method together with Newton's iterative technique (Rahman et al., 2010). The results have been presented for the chosen fluid of Prandtl number Pr = 0.71, but with different location of heater, length of the cavity, Rayleigh number, and heat generation parameter. An experimental and numerical study on laminar natural convection in a cavity heated from bottom wall due to an inclined fin was done (Varol et al., 2012). They observed that the heat transfer can be controlled by attaching an inclined fin on its wall. Previous investigations have merely focused on forced and natural convection heat transfer and the radiative mode of heat transfer was sometimes neglected because of the overwhelming amount of required computational resources. Besides, because of difficulties in obtaining accurate experimental data with small convective heat flux compared with radiative one, experimental data of natural convection in enclosures are generally less accurate than that of forced convection. Therefore, accurate numerical computations in combined heat transfer can be valuable. Some literatures try to show that radiation heat transfer has an important and significant effect on thermal system and cannot be neglected (Tan et al., 1991; Han et al., 2001). Furthermore, radiative heat transfer plays an important role on heat transfer in cavities. In the coupled radiation and natural convection, many works take only into account the effects of surface-to-surface radiation in order to reduce computational effort (Behnia et al., 1985; Behnia et al., 1985; Balaji et al., 1993; Velusamy et al., 2001; Mezrhab et al., 2006). The mathematical modeling aspects of coupled conductive and radiative heat transfer in the presence of absorbing, emitting and isotropic scattering gray medium within two-dimensional square enclosure was analyzed (Mahapatra et al., 2006). The gray participating medium was bounded by isothermal walls which were considered to be opaque, diffuse and gray. The effects of various influencing parameters i.e., radiation–conduction parameter, surface emissivity, single scattering albedo and optical thickness were illustrated. Combined heat transfer of natural convection and radiation in a 2D square cavity was studied numerically (lari et al., 2006). The continuity, momentum and energy equations were solved by the finite volume method and the radiative transfer equation by discrete ordinates method. The results showed that even under normal room conditions with a low temperature difference, the radiation plays a significant role on temperature distribution and flow pattern in the cavity. Also, several interesting effects of radiation were observed such as a sweep behavior on the isotherms, streamlines and velocity distributions of the cavity along the optical thickness and a reverse behavior on maximum stream function and convective Nusselt number at different values of Rayleigh number. However, only a very limited numerical and experimental works on combined radiation and forced convection heat transfer in a lid-driven cavity has been reported. In the present study, the problem of combined radiation and forced convection in a square lid-driven cavity filled with a participating medium and heated from high temperature lid on its top wall under the presence of heat generation source is studied. The analysis here employs discrete ordinates method (DOM) for computing radiative heat flux in participating media. Because, this method remains simple in expressions but retains important physical insights. On the other hand, it is clear from the literature review that less attention was made in analyzing radiative medium in lid-driven cavity using DOM. Therefore, the present work mainly aims the effect of radiation on forced convection heat transfer in a square lid-driven cavity under various conditions by using a precise numerical analysis with a broad range of the Reynolds number and different radiative parameters. To achieve this goal, a transient numerical procedure is offered to model the mentioned problem. The lid-driven cavity is considered as an absorbing-emitting and scattering media filled with gray gases. The finite difference method has been adopted to solve the set of governing equations and the radiative source term in the energy equation is computed from intensities field. The radiative convective model is validated by comparison with the well-documented results in open literature. This model is applied to determine the stream function, velocity and temperature distributions of the domain at different Reynolds numbers from the initial condition up to steady state one. Also, the effects of radiative parameters on the wall total heat fluxes are thoroughly investigated.

2. Analysis

2.1. Problem description

A schematic view of the lid-driven cavity by considering a non-uniform heat generation zone is shown in Figure 1. The width of the square cavity is denoted by H. The length of the geometry perpendicular to its plane is assumed to be long enough; hence, the problem is considered two dimensional. The upper horizontal wall moves on its own plane from left to right at constant speed (U) keeping all other walls fixed. The top wall is kept at a uniform hot temperature (T_h), while the other walls are kept at a uniform cold temperature (T_c). The surface emissivities are $\varepsilon = 1$ on the all boundaries and the working fluid is chosen as air with Prandtl number, Pr = 0.71. The non-uniform heat generation zone is situated in the region $x_1 < x < x_2$ with a parabolic variation in y-direction, such that maximum heat released at the centerline and the minimum value near the top and bottom walls. The contained gas in lid-driven cavity is assumed to be gray and isotropically emitting, absorbing and scattering media. The incident radiations are absorbed by the walls and the contained gas is heated by the convection heat transfer. The fluid flow is assumed to be laminar and incompressible, and all thermophysical properties of air inside the cavity are assumed to be constant.

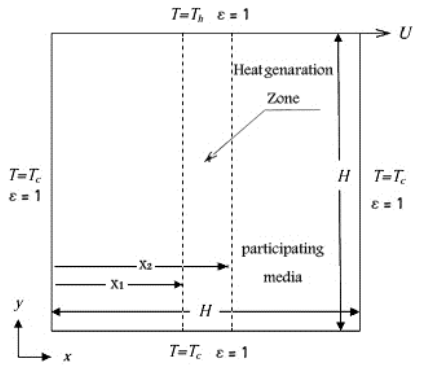

Fig 1. The configuration of the problem under consideration

2.2. Governing equations

Unsteady, two-dimensional, laminar, combined radiation and forced convection heat transfer of viscous incompressible fluid having constant properties, is studied here. Under these assumptions, governing equations are as follows (Bejan, 2004):

$$Continuity: \quad \frac{\partial u}{\partial x}+\frac{\partial v}{\partial y}=0, \tag{1}$$

$$x-momentum: \quad \frac{\partial u}{\partial t}+u\frac{\partial u}{\partial x}+v\frac{\partial u}{\partial y}=-\frac{1}{\rho}\frac{\partial p}{\partial x}+\nu\left(\frac{\partial^2 u}{\partial x^2}+\frac{\partial^2 u}{\partial y^2}\right), \tag{2}$$

$$y-momentum: \quad \frac{\partial v}{\partial t}+u\frac{\partial v}{\partial x}+v\frac{\partial v}{\partial y}=-\frac{1}{\rho}\frac{\partial p}{\partial y}+\nu\left(\frac{\partial^2 v}{\partial x^2}+\frac{\partial^2 v}{\partial y^2}\right), \tag{3}$$

$$Energy: \quad \frac{\partial T}{\partial t}+u\frac{\partial T}{\partial x}+v\frac{\partial T}{\partial y}=\alpha\left(\frac{\partial^2 T}{\partial x^2}+\frac{\partial^2 T}{\partial y^2}\right)+\dot{Q}(y)\delta(x)-\frac{1}{\rho c_p}\nabla.q_r. \tag{4}$$

These equations are written in dimensionless forms by the following nondimensional groups:

$$U=uH/\alpha,\ V=vH/\alpha,\ \eta_x=x/H,\ \eta_y=y/H,\ t^*=t\alpha/H^2$$

$$\theta=(T-T_c)/\Delta T,\ \prod_1=\frac{\dot{Q}H^2}{k\Delta T},\ \prod_2=k/H\sigma T_c^3,\ P=pH^2/\rho\alpha,\ Q=q/\dot{Q}H$$

$$\Psi=\psi/\alpha,\ pr=\nu/\alpha,\ \phi=\Delta T/T_c,\ I^*=I/\sigma T_C^4$$

Substitution of dimensionless variables into equations (1)-(4) leads to:

$$Continuity: \quad \frac{\partial U}{\partial \eta_x}+\frac{\partial V}{\partial \eta_y}=0, \tag{5}$$

$$x-momentum: \quad \frac{\partial U}{\partial t^*}+U\frac{\partial U}{\partial \eta_x}+V\frac{\partial U}{\partial \eta_y}=-\frac{\partial P}{\partial \eta_x}+\Pr\left(\frac{\partial^2 U}{\partial \eta_x^2}+\frac{\partial^2 U}{\partial \eta_y^2}\right), \tag{6}$$

$$y-momentum: \quad \frac{\partial V}{\partial t^*}+U\frac{\partial V}{\partial \eta_x}+V\frac{\partial V}{\partial \eta_y}=-\frac{\partial p}{\partial \eta_y}+\Pr\left(\frac{\partial^2 V}{\partial \eta_x^2}+\frac{\partial^2 V}{\partial \eta_y^2}\right), \tag{7}$$

$$Energy: \quad \frac{\partial \theta}{\partial t^*}+U\frac{\partial \theta}{\partial \eta_x}+V\frac{\partial \theta}{\partial \eta_y}=\left(\frac{\partial^2 \theta}{\partial \eta_x^2}+\frac{\partial^2 \theta}{\partial \eta_y^2}\right)+\prod_1\delta(x)-\frac{1}{\prod_2\phi}\nabla^*.Q_r. \tag{8}$$

The term $\delta(x)$ is the delta function defined as unity for $x_1 \le x \le x_2$ and zero elsewhere. The heat source term $\nabla.q_r$ due to radiation in energy equation, is calculated from the radiant intensity field. A general equation for radiant intensity in emitting-absorbing and scattering gray medium presented as follow (Modest, 1993):

$$(\Omega.\nabla)I(r,\Omega) = K_a I_b(r) - \beta I + \frac{\sigma_s}{4\pi}\int_{4\pi} I(r,\Omega')\phi(\Omega'\to\Omega)d\Omega' \qquad (9)$$

where σ is the scattering coefficient and $\Phi(\Omega'\to\Omega)$ is the scattering phase function. For the diffusely reflecting walls, the radiative transfer equation (RTE) is subject to the following boundary conditions:

$$I(r_w,\hat{s}) = \varepsilon(r_w)I_b(r_w) + \frac{\rho(r_w)}{\pi}\sum_{\hat{n}.\hat{s}_j<0} I(r_w,\hat{s}_j)\left|\hat{n}.\hat{s}_j\right|w_j \qquad \text{for:} \quad \hat{n}.\hat{s}_i > 0 \qquad (10)$$

where ε and ρ are wall emissivity and reflectivity of the surface, respectively. It is obvious that the integro-differential Eq. (10) does not have analytical solution, so the researchers represented different approximate solutions for solving this equation. Amongst many numerical methods of solving RTE, the discrete ordinate method or S_N -Approximation is widely used by investigators. DOM is a wonderful and applicable tool in transforming the RTE into a set of ordinary differential equations for n different directions, $\hat{s}_i = 1,2,...,n$. Once the intensities have been determined in the desired directions, integrated quantities can be readily calculated. For two dimensional problems, RTE became as follows (Fiveland, 1984):

$$\zeta^m \frac{\partial I^m}{\partial \eta_x} + \mu^m \frac{\partial I^m}{\partial \eta_y} = -\beta I^m + \beta[(1-\omega)I_b(r) + \frac{\omega}{4\pi}\sum_{m'} w^{m'} I^{m'}] \qquad (11)$$

The following equation can be obtained for computing radiant intensity by differentiation of the above equation:

$$I^m_{(j,k)} = \frac{I^m_x + I^m_y + \sigma_a I_b + S^m}{\sigma_e + x^m sign(x^m) + y^m sign(y^m)} \qquad (12)$$

By determination of the intensities in the desired directions, integrated quantities can be computed. Consequently, the radiative heat flux inside the medium may be calculated as follows:

$$q(r) = \int_{4\pi} I(r,\hat{s})\hat{s}d\Omega \approx \sum_{i=1}^{n} w_i I_i(r)\hat{s}_i \qquad (13)$$

The effect of thermal radiation is taken into consideration in Eq. (4) as the divergence of the heat flux, that can be computed by:

$$\nabla.q_r = k_a[4\pi I_b(r) - \sum_{i=1}^{n} I(r,s_i)w_i] \qquad (14)$$

the non-dimensional form of Eqs. (9) and (15) can be written as follows:

$$Divergence\ of\ the\ radiative\ flux: \quad \nabla^*.Q_r = \tau(1-\omega)[4(\theta\phi+1)^4 - \int_{4\pi} I^* d\Omega] \qquad (15)$$

$$RTE: \qquad \frac{1}{\tau}(\Omega.\nabla^*)I^* = \frac{(1-\omega)}{\pi}(\theta\phi+1)^4 - I^* + \frac{\omega}{4\pi}\int_{4\pi} I^*\Phi d\Omega' \qquad (16)$$

The convective, radiative and overall heat fluxes at the walls are calculated as follows:

Convective heat flux: $q_c = -k\frac{\partial T}{\partial x} \quad or \quad -k\frac{\partial T}{\partial y}$ (17)

Radiative heat flux: $q_r = \pi I(r_w,\hat{s}) = \pi\varepsilon(r_w)I_b(r_w) + \rho(r_w)\sum_{\hat{n}.s_j<0} I(r_w,\hat{s}_j)\left|\hat{n}.\hat{s}_j\right|w_j \quad (for \quad \hat{n}.\hat{s}_i > 0)$ (18)

Overall heat flux: $q_{ov} = q_c + q_r$ (19)

Equations (5) - (8) and Eq. (15) should be solved by appropriate boundary conditions. In accordance with the problem description, the initial and boundary conditions after non-dimensionalization can be written as follows:

$$U = V = 0, \quad \theta = 0 \quad (for \quad t = 0)$$

$$at \begin{cases} \eta_y = 1, \\ 0 \le \eta_x \le 1 \end{cases} \qquad U = 1, V = 0, \ \theta = 1 \qquad (for \quad t > 0)$$

$$at \begin{cases} \eta_y = 0, \\ 0 \le \eta_x \le 1 \end{cases} \qquad U = V = 0, \ \theta = 0 \qquad (for \quad t > 0)$$

$$at \begin{cases} \eta_x = 0,1 \\ 0 \le \eta_y \le 1 \end{cases} \qquad U = V = 0, \ \theta = 0 \qquad (for \quad t > 0)$$

For solving the radiative transfer equation, the following two boundary conditions are employed at the side boundaries $\eta_x = 0,1$:

$$at \quad \eta_x = 0 \qquad I^* = \frac{\varepsilon_w \theta_w^4}{\pi} + \frac{1-\varepsilon_w}{\pi} \sum_{\zeta_j < 0} I_j^* \left|\zeta_j\right| w_j \qquad (for \quad \zeta_i > 0)$$

$$at \quad \eta_x = 1 \qquad I^* = \frac{\varepsilon_w \theta_w^4}{\pi} + \frac{1-\varepsilon_w}{\pi} \sum_{\zeta_j > 0} I_j^* \left|\zeta_j\right| w_j \qquad (for \quad \zeta_i < 0)$$

Finally, the following two boundary conditions are employed for the top and bottom walls, $\eta_y = 0,1$:

$$at \quad \eta_y = 0 \qquad I^* = \frac{\varepsilon_w \theta_w^4}{\pi} + \frac{1-\varepsilon_w}{\pi} \sum_{\mu_j < 0} I_j^* \left|\mu_j\right| w_j \qquad (for \quad \mu_i > 0)$$

$$at \quad \eta_y = 1 \qquad I^* = \frac{\varepsilon_w \theta_w^4}{\pi} + \frac{1-\varepsilon_w}{\pi} \sum_{\mu_j > 0} I_j^* \left|\mu_j\right| w_j \qquad (for \quad \mu_i < 0)$$

3. SOLUTION TECHNIQUE AND VALIDATION

Navier–Stokes and energy equations have been solved numerically based on the finite difference method using a staggered grid system. Central difference quotients were used to approximate the second derivative in both x- and y-directions (Patankar, 1980). To account for the velocity–pressure coupling, the projection method is adopted. Also the DOM is employed to solve RTE via iterative technique.

The sequence of calculations can be stated as follows:

1. A first approximation for each dependent variable, velocity, temperature, and intensity field is assumed.
2. The finite difference form of RTE is solved for obtaining the value of I, Q and $\nabla.Q$ at each nodal point using S_6-Approximation until convergence.
3. The momentum and energy equations for the flow field are solved to find the velocity and temperature fields at each time step.
4. RTE is solved for updating the values of I, Q and $\nabla.Q$ at each time step.
5. Repeat 2–4 for successive time steps until the velocity and temperature fields achieve steady state condition.

To check the convergence of the sequential iterative solution, the sum of the absolute differences of the solution variables between two successive iterations has been calculated. When this summation fall the convergence criterion as follows, convergence is obtained.

$$Max \left| \frac{\lambda_p^k - \lambda_p^{k-1}}{\lambda_p^k} \right| \le 10^{-5}$$

Where λ can be I^*, U, V and θ.

A couple of measures were introduced to assess the validity of the present numerical scheme. First, the sensitivity of the numerical outcome was examined by systematically increasing the mesh size until further refinement of the mesh size agreed to better than one percent difference in the computational solution. Table.1 shows the amount of overall heat flux on the middle of cavity walls for given conditions $(T_T = 773K, T_B = T_L = T_R = 373K)$ at $\mathrm{Re} = 100$. A mesh size of

58×58 was found adequate to simulate the flow and thermal responses of the problem under consideration. Therefore, this grid size is used in all subsequent simulations.

Table. 1 Amount of overall heat flux (w/m^2) on the middle of walls for grid independence examination

No.	Mesh size	$q_{ov,T}(-)$	$q_{ov,B}(-)$	$q_{ov,L}(-)$	$q_{ov,R}(-)$
1	42×42	2508.74	652.32	836.74	7.43
2	48×48	2508.12	651.76	836.22	7.06
3	58×58	2507.54	651.42	835.65	6.66
4	64×64	2507.51	651.05	835.41	6.86

$(T_T = 773K, T_B = T_L = T_R = 373K)$

$(\varepsilon_T = \varepsilon_B = \varepsilon_L = \varepsilon_R = 1, \omega = 0.5, k_a = 50(m^{-1}), \mathrm{Re} = 100)$

The second measure for the validation process composed of comparing the outcome of the numerical code against a reliable documented work in literature. In order to validate the computational results, two test cases have been considered.

At the first case, the present results for the fluid flow in a lid-driven cavity are compared with those obtained by theoretical data (Ghia et al., 1982), for the same conditions. For this purpose, the top wall is constantly slide to the right at constant velocity. This numerical method has been performed for the lid-driven cavity filled by pure fluid. Figure 2(a) and 2(b) show computed velocity distributions at the mid-plan of the domain for a flow at Re = 400. The values of maximum and minimum velocities and also their locations in these works are closed to each other. However, the agreement between the present results with those obtained by Ghia et al. is satisfactory.

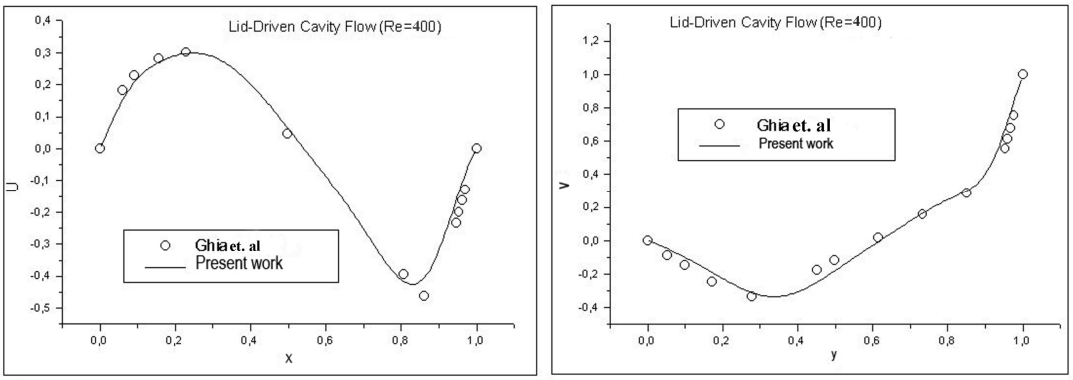

(a) y=H/2 (b) x=H/2

Fig 2. Distributions of x- and y- velocity components at the mid-plan inside the cavity

To validate the present computations in solving the RTE by DOM, there is no any theoretical result in laminar forced convection flow inside a lid-driven cavity. But there is a research work about analysis of combined conduction- radiation heat transfer in presence of participating media (Mahapatra et al., 2006). Therefore, second validation is done based on the results of these investigators. In that study, a mathematical modeling carried out for analyzing of coupled conductive-radiative heat transfer in the presence of absorbing, emitting and isotropic scattering gray medium within two-dimensional square enclosure. Fig. 3 shows a simplified schematic of the cavity with $L_x = L_y = 1m$ that considered at this investigation. The left side surface is hot at nondimensional temperature $\theta = 1$ and other surfaces are cold at temperature $\theta = 0.5$, while all boundaries are black. In Fig. 4 the dimensionless temperature distribution for the radiation-conduction parameter $(RC = \sigma T_h^3 H/k)$ equal to 10 is presented. They showed that, the radiation-conduction parameter should be equal or smaller than unity to require a radiation heat transfer calculation. As RC decreases, radiation plays a more significant role than conduction. Therefore, as RC decreases, a steeper temperature gradient is formed at both end walls (right and left surfaces) and the medium temperature increases as shown in Figure 4. The results for the mid-plan temperature distribution are in very good agreement with those presented by Mahapatra.

The consistency between these results shows the accuracy of the present numerical procedure. At the present work, a numerical study has been performed to explore the combined radiation and forced convection heat transfer characteristics of participating medium contained in a lid-driven cavity, while a non-uniform heat generation zone inside the media presents.

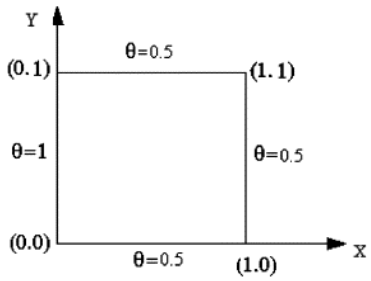

Fig. 3 The geometry of second test case

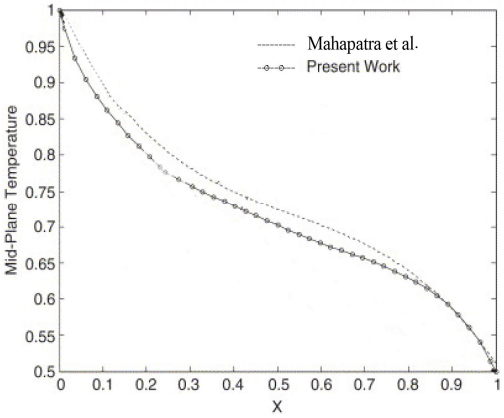

Fig. 4 Comparison of mid-plan temperature in cavity with theoretical results (Mahapatra et al., 2006).

$$(\theta_L = 1,\ \theta_B = \theta_T = \theta_R = 0.5)$$

$$(\varepsilon_T = \varepsilon_B = \varepsilon_L = \varepsilon_R = 1, \omega = 0.5, \tau = 1)$$

4. RESULTS AND DISCUSSION

Combined radiation and forced convection heat transfer in a lid-driven square cavity filled with emitting, absorbing and scattering media and the presence of a heat generation zone are examined. At this present, based on the discrete ordinate method, the effect of various influencing parameters, such as Reynolds number, scattering albedo and location of heat generation zone inside the cavity has been investigated. For this purpose, temperature contours and heat flux distributions on lid-driven walls at various conditions are illustrated and the numerical results are plotted in Figures 5 to 14 along many curves. The non-dimensional parameters for this test case are given in Table 2.

Table. 2 Non–dimensional parameters of the test case

Parameter	value
U	1
θ_h	1
θ_c	0
$\rho u c T_c / \dot{Q} H^2$	0.02
$\Pi_1 = \dot{Q} H^2 / k \Delta T$	6×10^4
$\Pi_2 = k / H \sigma T_c^3$	0.001

In order to obtain the radiation effect in convection flow, the contours of temperature inside cavity with and without considering the radiation term in energy equation are shown in Figure 5. The center of generation zone is placed at the cavity center while its thickness is equal to 0.1 H. The effect of radiation on thermal behavior of the system can be found if one compares Figures 5(a), (b) and (c) with 5(d), (e) and (f) at the same time steps. The distributions of temperature contours at different times are plotted in Figure 5. It is seen that in all time steps, radiation heat transfer causes more uniform temperature inside the thermal system, especially at the start of unsteady operation of system, with this fact that the temperature patterns in both cases considering radiation effect and neglecting it are similar to each other. In all of the plotted curves in Figure 5, there are high temperature regions near to the top wall and inside the heat generation zone, such that the effect of moving wall from left to right causes a high temperature zone in the left part of the cavity in comparison to the right part. This is because of the fluid flow pattern in the cavity and the effect of forced convection heat transfer

inside the thermal system. If one compares the temperature contours plotted in Figure 5, it can be found that the value of maximum temperature in the cavity at the start of system operation increases while the radiation heat transfer is considered into account. This is because the existence of heat generation zone and absorbing more thermal energy by the participating media initially. Comparison of Figures 5(c) and 5(d) illustrate similar pattern for isotherm lines at steady-state condition, with this fact that the radiative effect decreases the value of maximum temperature inside the cavity. Finally Figure 5 illustrated that the value of temperature gradient near to the hot wall (top surface) decreases with increasing in time. So, as the thermal system moves from its initial operation time to its steady state condition, the convection heat flux at the hot wall decreases and its maximum value takes place just at the start of system operation.

The distributions of radiative heat flux on the boundary surfaces including top wall which has high temperature and three other walls which are maintained at low temperature are plotted in Figure 6. This figure shows that the amount of heat flux on all boundaries because of radiation is high at the start of system operation and then it decreases by spending time up to steady-state condition.

Among all of the cavity walls, the bottom and right walls have small radiative heat flux, because they are maintained at low temperature. If one compares Figures 6(c) and 6(d) with each other, it can be seen that although both of the left and right walls are cold surfaces with temperature Tc, but the left one has radiative heat flux in comparison to the right one. This is due to the unsymmetric fluid flow pattern and then the temperature field inside the cavity because of the top wall movement from left to right direction. It is clear that in combined radiation and forced convection thermal systems, the overall heat flux on the walls are due to both radiant and convection, such that $q_{ov} = q_{conv} + q_{rad}$. The variations of this parameter along the cavity walls are shown in Figure 7. It is seen that the value of overall heat flux on all boundary surfaces varies by time such that for bottom and left walls, q_{ov} has its maximum values at the start of system operation, but for the top and right walls, the opposite behavior is seen. The explanation this thermal behavior is very difficult because of the non-linear behavior of radiative heat transfer, especially when it is combined to other modes of heat transfer. In order to study the effects of Reynolds number and scattering coefficient on the performance of thermal system, the distributions of temperature along the x-axis at the mid-plan $(y = H/2)$ are plotted in Figure 8. This figure shows that an increase in the value of Reynolds number leads to slightly temperature increase inside the cavity. Beside, comparison between the curves plotted in Figure 8 depicts that the media scattering coefficient has not considerable effect on temperature distribution.

As it was noted before, in the present case study, a rectangular heat generation zone with the thickness 0.1H and along the y-axis through the cavity presents. In Figure 10, the effect of heat generation zone location on the thermal behavior of the system is studied by plotting isotherm lines at three different values of x_c in the cases of considering radiation effect and neglecting it. It is seen that isotherm distributions have similar patterns in two cases including presence and absence of radiation, such that the maximum value of temperature takes place inside the heat generation zone, with this fact that radiation effect causes slightly increase in the value of maximum temperature.

In Figure 9, the effects of the same parameters Re and ω on overall heat flux distributions along the cavity walls are carried out. It is seen that the wall heat flux has increasing trend by increasing in Reynolds number, especially for the left, top and bottom walls. This is due to this fact that there is a region with high convection rate closed to these surfaces wall which is generated by moving the top surface of cavity. Besides, Figure 9 illustrates that the overall surface heat flux on the right wall is not affected by ω, while for other walls, high overall heat flux happens under small values for scattering coefficient.

To study more about the effect of x_c on temperature distribution inside the cavity, the variations of fluid temperature at the mid-plan along the x-axis are plotted in Figure 11 at three different values of x_c. This figure shows that the maximum temperature occurs at the heat generation zone, such that for all values of x_c, temperature distributions have similar patterns. Besides, it is seen that radiation causes slightly increase in the value of gas temperature.

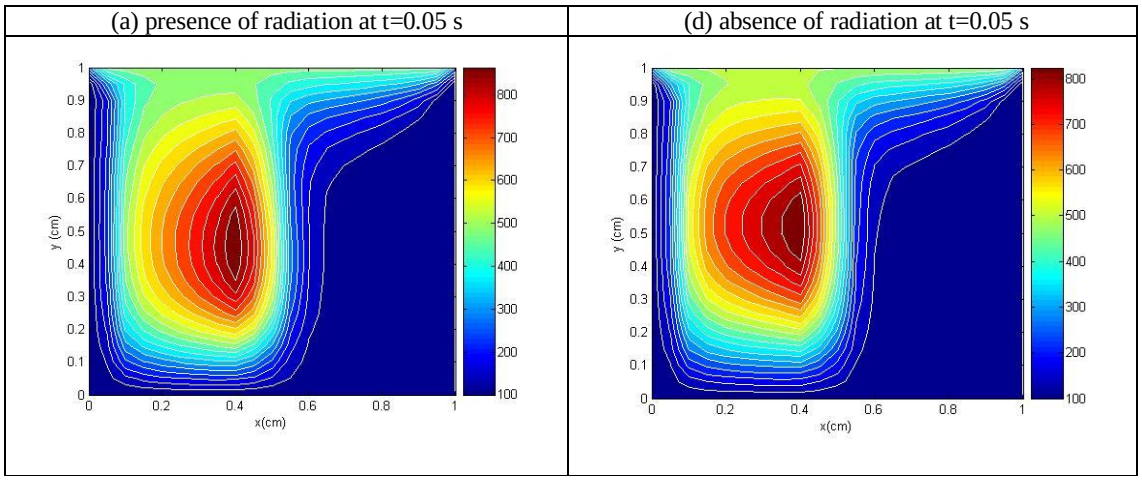

(b) presence of radiation at t=0.15 s	(e) absence of radiation at t=0.15 s
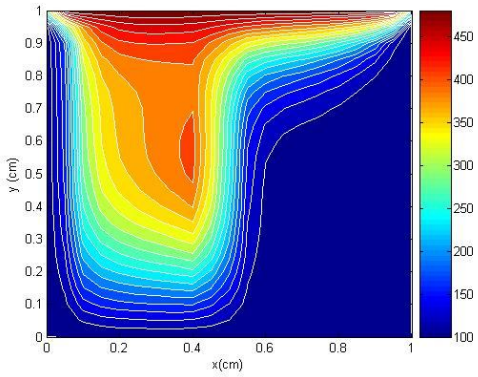	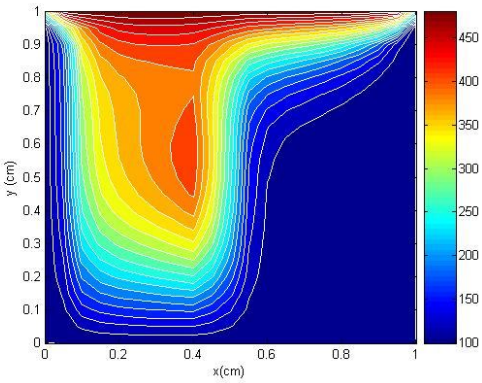
(c) presence of radiation at t=0.25 s	(f) absence of radiation at t=0.25 s

Fig. 5 Comparison of temperature contours at presence and absence of radiation effect in cavity at two different time steps for $\omega = 0.5, k_a = 50(m^{-1}), \mathrm{Re} = 100, x_c = H/2$

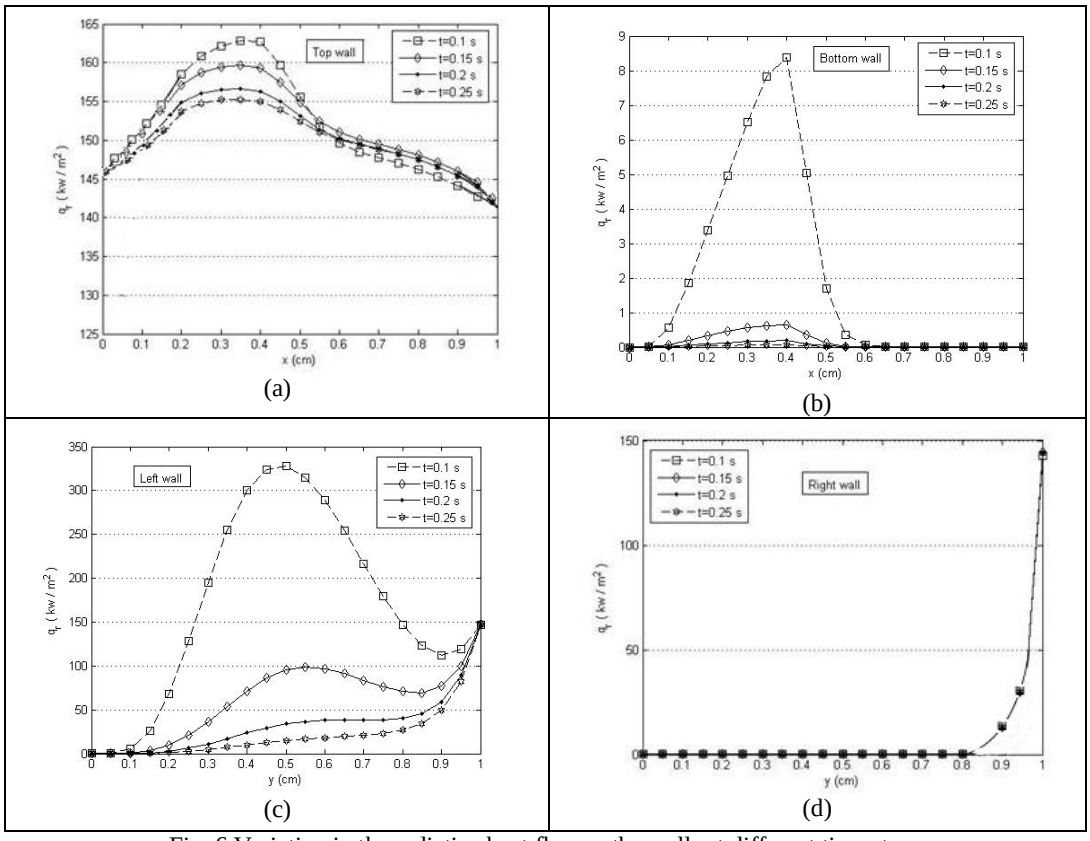

Fig. 6 Variation in the radiative heat flux on the walls at different time steps for $\omega = 0.5, k_a = 50(m^{-1}), \mathrm{Re} = 100, x_c = H/2$

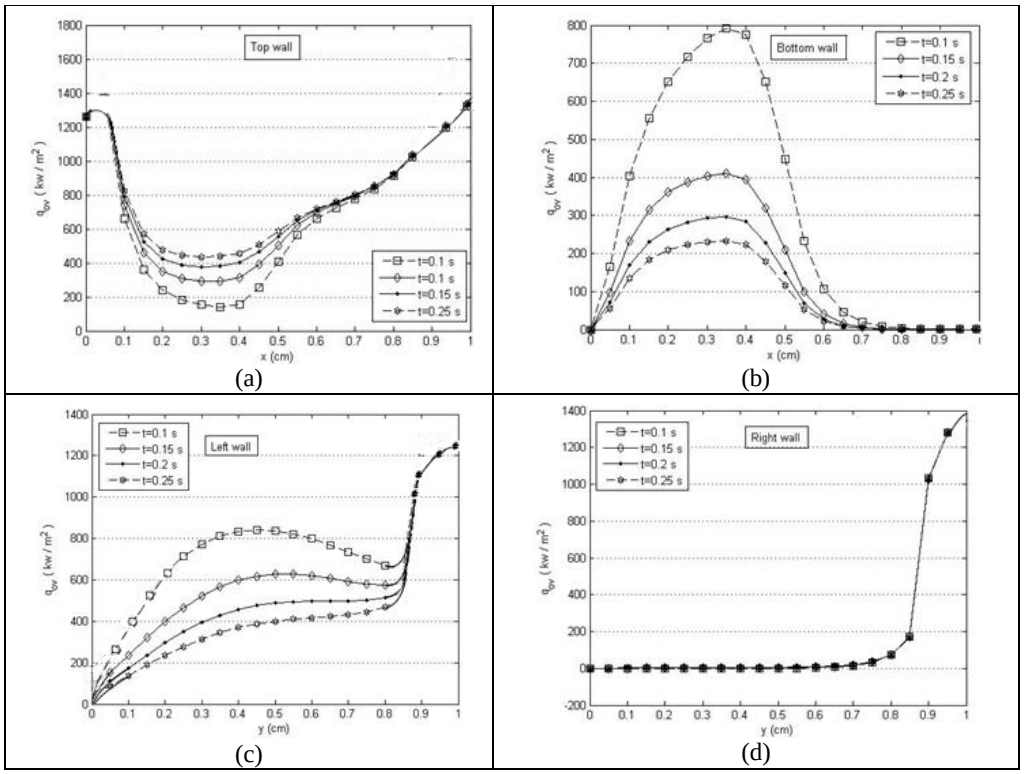

(a) (b)

(c) (d)

Fig. 7 Variation in the overall heat flux on the walls at different time steps for $\omega = 0.5, k_a = 50\,(m^{-1}), \mathrm{Re} = 100, x_c = H/2$

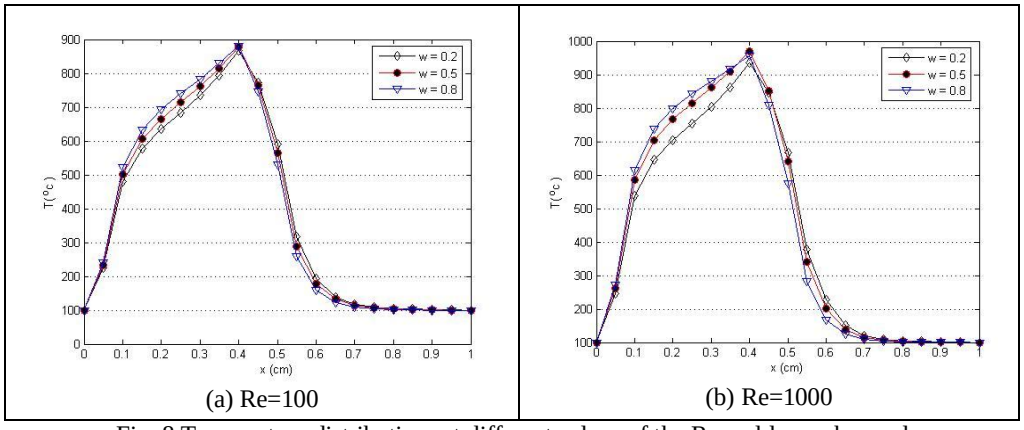

(a) Re=100 (b) Re=1000

Fig. 8 Temperature distributions at different values of the Reynolds number and scattering albedo at y=H/2 $(t = 0.1\ s, k_a = 50\,(m^{-1}), x_c = H/2)$

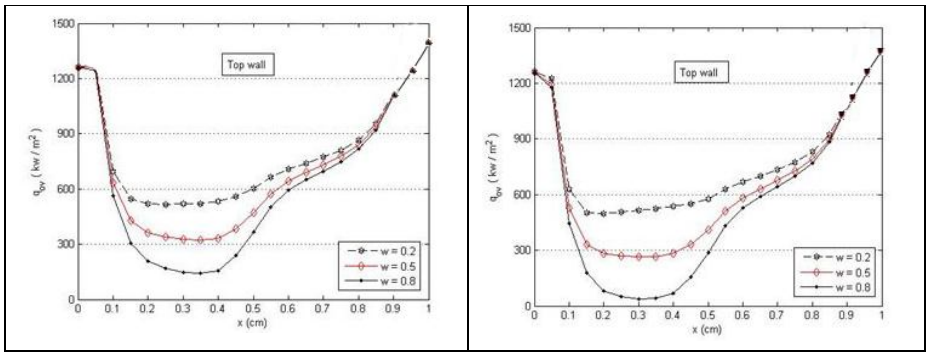

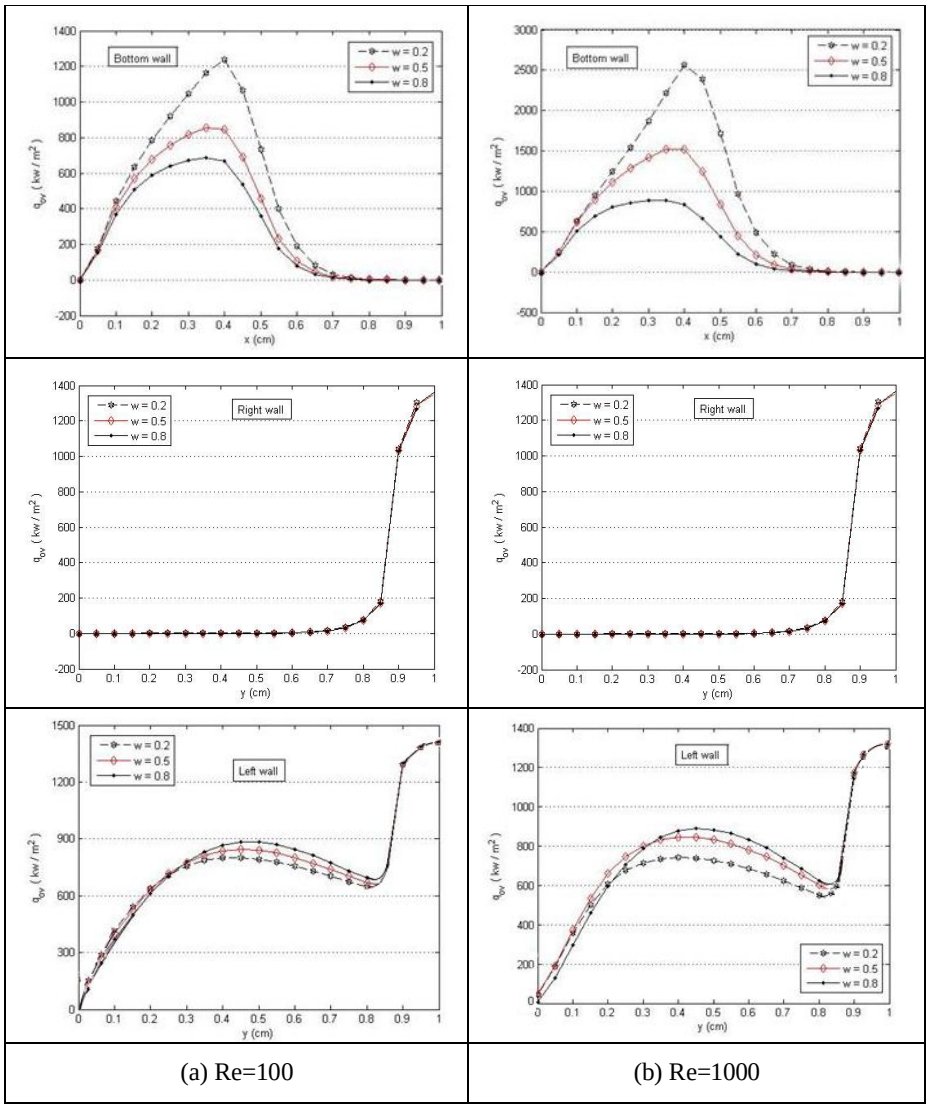

(a) Re=100 (b) Re=1000

Fig. 9 Variation in the overall heat flux at three different scattering albedo for two different Re values $(t = 0.1\,s, k_a = 50\,(m^{-1}), x_c = H/2)$

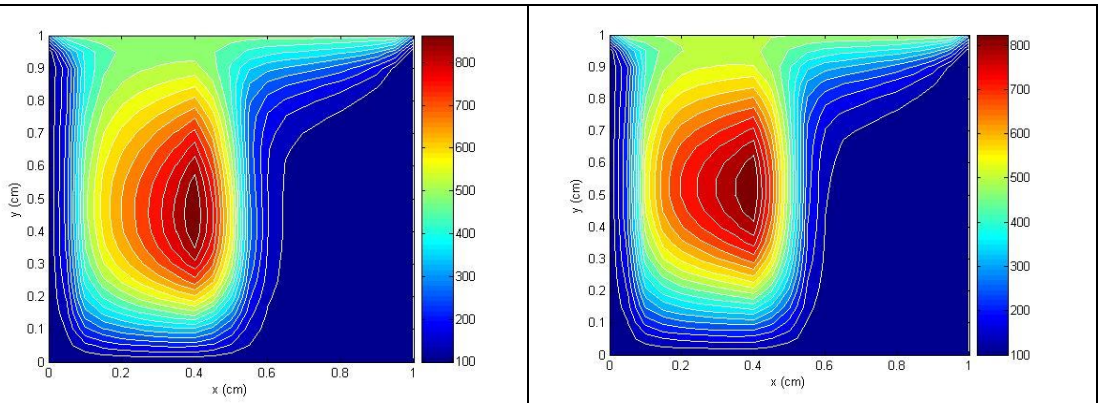

(a) $x_c = H/4$ (d) $x_c = H/4$

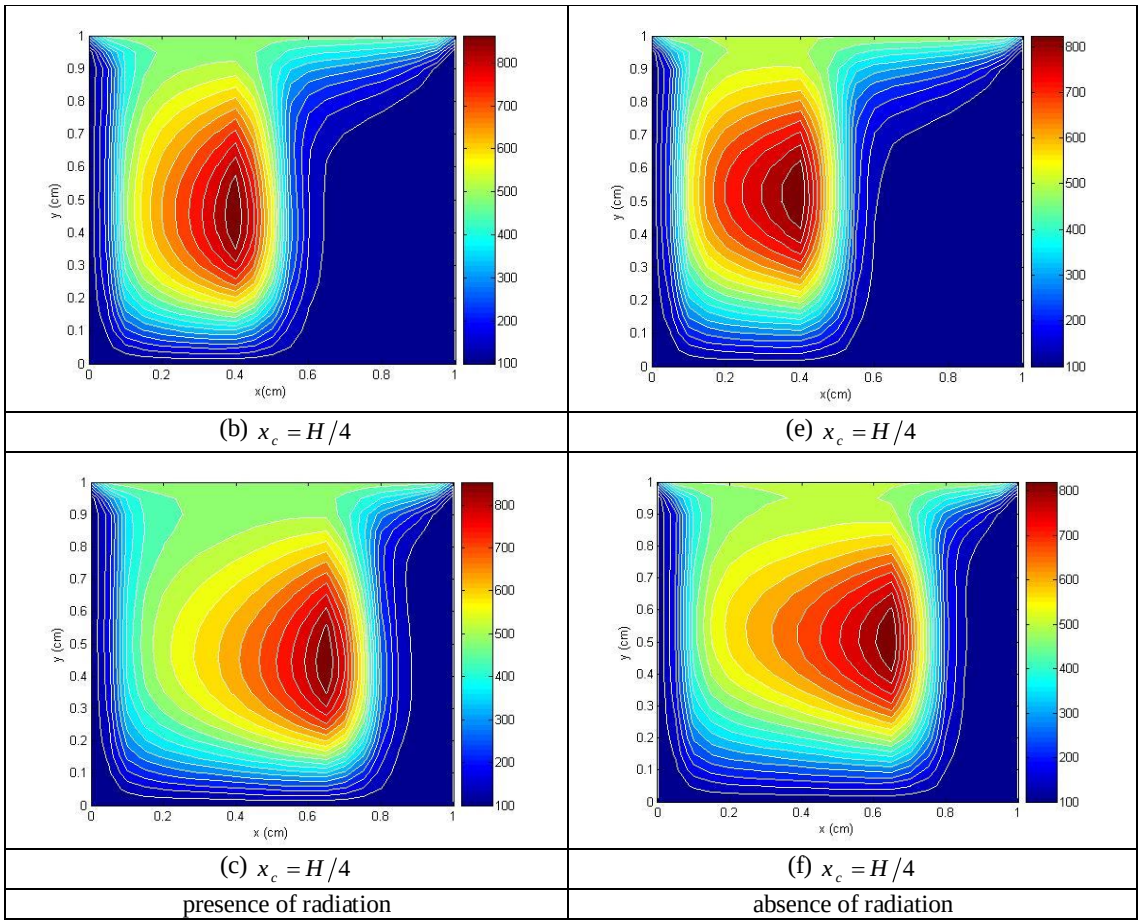

(b) $x_c = H/4$ | (e) $x_c = H/4$

(c) $x_c = H/4$ | (f) $x_c = H/4$

presence of radiation | absence of radiation

Fig. 10 Comparison of temperature contours at presence and absence of radiation in cavity at three different location of heat generation zone for $t = 0.1\,s, \omega = 0.5, k_a = 50\,(m^{-1}), \mathrm{Re} = 100$

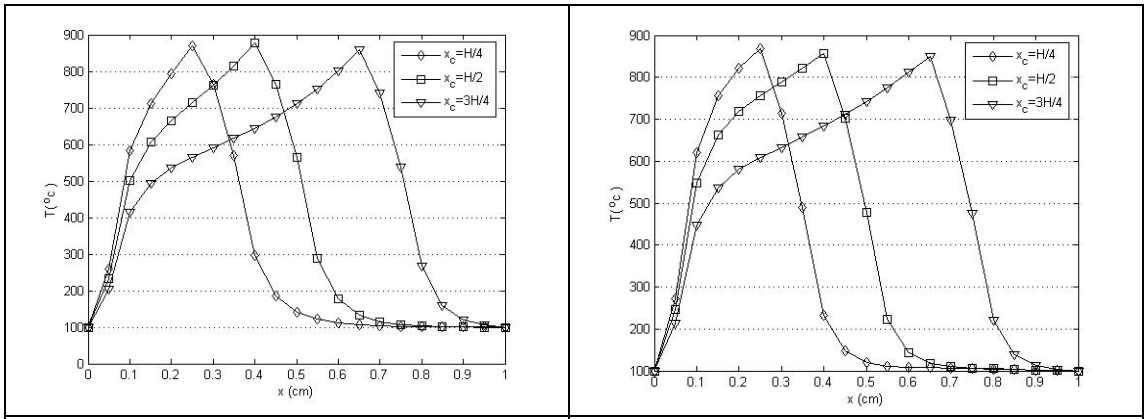

(a) presence of radiation | (b) absence of radiation

Fig. 11 Comparison of distributions of gas temperature in mid-plan along the cavity (y=H/2) at presence and absence of radiation in cavity at three different location of heat generation zone for $t = 0.1\,s, \omega = 0.5, k_a = 50\,(m^{-1}), \mathrm{Re} = 100$

CONCLUSIONS

A numerical investigation has been made on the 2-D lid-driven cavity filled with participating media by considering a non-uniform heat generation zone to obtain the thermal characteristics of this system. The discrete ordinates method was used to transform the equation of radiative transfer to a set of partial differential equations, which were numerically solved simultaneously with the energy equation. Results for the temperature contours, mid-plan temperature distribution and overall heat flux distributions on the walls were obtained for different parameters like the Reynolds number, scattering coefficient and location of heat generation zone. It was found these parameters have great effects on thermal behavior of such systems.

REFERENCES

1. Aluria, Y. and Torrance, K. E., 1986, Computational Heat Transfer, Hemisphere, Washington.
2. Moallemi, M.K. and Jang, K.S., 1992, Prandtl number effects on laminar mixed convection heat transfer in a lid-driven cavity, Heat Mass Transfer, 35: 1881–1892.
3. Kuhlmann, H.C., Wanschura, M. and Rath, H.J., 1997, Flow in two sided lid-driven cavities: non-uniqueness, instabilities, and cellular structures, Fluid Mech., 336: 267–299.
4. Chamkha, A. J., 2002, Hydro-magnetic combined convection flow in a vertical lid-driven cavity with internal heat generation or absorption, Numer. Heat Transfer, Part A, 41: 529-546.
5. Ji, T.H., Kim, S. Y. and Hyun, J. M., 2007, Transient mixed convection in an enclosure driven by sliding lid, Heat and Mass Transfer, 43: 629-938.
6. Khanafer, K., Vafai, K. and Lightstone M., 2003, Buoyancy-driven heat transfer enhancement in a two-dimensional enclosure utilizing nanofluids, Heat and Mass Transfer. 19: 3639–3653.
7. Das, P.K., Mahmud, S., 2003, Numerical investigation of natural convection inside a wavy enclosure, Thermal Science, 42: 397– 406.
8. Buscaglia, G.C. and Dari, Enzo, A., 2003, Numerical investigation of flow through a cavity with internal heat generation, Numerical Heat Transfer, Part A, 43: 525–541.
9. Gau, G. and Sharif, M. A. R., 2004, Mixed convection in rectangular cavities at various aspect ratios with moving isothermal side walls and constant flux heat source on the bottom wall, Thermal Sciences, 43: 465-475.
10. Oztop, H.F., and Dagtekin I., 2004, Mixed convection in two-sided lid-driven differentially heated square cavity, Int. J. Heat Mass Transfer, 47: 1761–1769.
11. Al-Amiri, A., Khanafer, K. and Bull, J., 2007, Effect of sinusoidal wavy bottom surface on mixed convection heat transfer in a lid-driven cavity, Heat and Mass Transfer, 50: 1771–1780.
12. Mohammed, H., A., 2008, Laminar mixed convection heat transfer in a vertical circular tube under buoyancy assisted and opposed flows, Energy Conversion and Management, 49: 2006–2015.
13. Abu-Nada, E, Masoud, Z, Oztopd, H., and Campo, A., 2010, Effect of nanofluid variable proper-ties on natural convection in enclosures. Thermal Scinces, 49: 479–491.
14. Aminossadatia, S. M. and Ghasemi, B., 2009, Natural convection cooling of a localized heat source at the bottom of a nanofluid-filled enclosure. European Journal of Mechanics, 28: 630-640.
15. Aldawody, D. A., and Elbashbeshy E. M. A., 2011, Heat transfer over an unsteady stretching surface in a micro polar fluid in the presence of magnetic field and thermal radiation. Canadian J. Physics, 89: 295-298.
16. Turkyilmazoglu, M., 2011, Thermal radiation effects on the time- dependent MHD permeable flow having variable viscosity. Thermal Science, 50: 88-96.
17. Raisi, A., Ghasemi, B., and Aminossadati, S.M., 2011, A numerical forced convection of laminar nanofluid in a micro channel with both slip and no-slip condition, Numerical Heat Transfer; Part A: Applications, 59: 114–129.
18. Rahman, M. M., Mamun, M. A. H. Billah, M. M. and Saidur R., 2010, Natural convection flow in a square cavity with internal heat generation and a flush mounted heater on a side wall. Naval Architecture and Marine Engineering, 7: 37–50.
19. Varol, Y., Oztop, H.F., Ozgen, F., Koca, A., 2012, Experimental and numerical study on laminar natural convection in a cavity heated from bottom due to an inclined fin, Heat Mass Transfer, 48: 61–70.
20. Behnia, M. Reizes, J.A. and de Vahl Davis G., 1985, Natural convection in a cavity with a window, in: Proceedings of the AIAA 20th Thermophysics Conference, Williamsburg, VA, 19–21.
21. Behnia, M. Reizes, J.A. and de Vahl Davis G., , 1985, Natural convection in a rectangular slot with convective–radiative boundaries, in: Proceedings of the National Heat Transfer Conference.
22. Balaji, C., and Venkateshan, S.P., 1993, Interaction of surface radiation with free convection in a square cavity, Heat Fluid Flow, 14: 260–267.
23. Velusamy, K., Sundararajan, T. and Seetharamu, K.N., 2001, Interaction effects between surface radiation and turbulent natural convection in square and rectangular enclosures, Heat Transfer. 123: 1062–1070.
24. Mezrhab, H. Bouali, Amaoui, H., Bouzidi, M. Computation of combined natural-convection and radiation heat-transfer in a cavity having a square body at its center, Appl. Energy, 2006, 83, p. 1004–1023.
25. Mahapatra, S.K., Dandapat and B.K., Sarkar, A., 2006, Analysis of combined conduction and radiation heat transfer in presence of participating medium by the development of hybrid method. Quantitative Spectroscopy and Radiative Transfer, 102: 277-292.
26. Lari, K., Baneshi, M., Gandjalikhan Nassab, S.A., Komiya, A. and Maruyama S., 2011, Combined heattransfer of radiation and natural convection in a square cavity containing participating gases, Int. J. Heat and Mass Transfer, 54: 5087–5099.
27. Tan, Z., and Howell, J.R., 1991, Combined radiation and natural convection in a two-dimensional participating square medium. Heat Mass Transfer, 34: 785–793.
28. Han, C.Y., and Baek, S.W., 2000, The effects of radiation on natural convection in a rectangular enclosure divided by two partitions, Numer. Heat Transfer Part A, 37: 249–270.
29. Bejan, A., 2004, Convection heat transfer, New Jersey: John Wiley & Sons Inc.
30. Modest, M. F., 1993, Radiative Heat Transfer, McGraw-Hill, New York.
31. Fiveland, W. A., 1984, Discrete- ordinates solution of the radiative transport eqution. Heat Transfer, 106: 699 - 706.
32. Patankar, S.V., 1980, Numerical Heat Transfer and Fluid Flow, Hemisphere Publishing Corporation, Taylor and Francis Group, New York.